Cochlear partition anatomy and motion in humans differ from the classic view of mammals

Stefan Raufer[a,b,1], John J. Guinan Jr.[a,b,c], and Hideko Heidi Nakajima[a,b,c]

[a]Eaton-Peabody Laboratories, Massachusetts Eye and Ear, Boston, MA 02114; [b]Speech and Hearing Bioscience and Technology Program, Harvard University, Cambridge, MA 02138; and [c]Department of Otolaryngology, Harvard Medical School, Boston, MA 02115

Edited by Christopher A. Shera, University of Southern California, Los Angeles, CA, and accepted by Editorial Board Member Thomas D. Albright June 6, 2019 (received for review January 16, 2019)

Mammals detect sound through mechanosensitive cells of the cochlear organ of Corti that rest on the basilar membrane (BM). Motions of the BM and organ of Corti have been studied at the cochlear base in various laboratory animals, and the assumption has been that the cochleas of all mammals work similarly. In the classic view, the BM attaches to a stationary osseous spiral lamina (OSL), the tectorial membrane (TM) attaches to the limbus above the stationary OSL, and the BM is the major moving element, with a peak displacement near its center. Here, we measured the motion and studied the anatomy of the human cochlear partition (CP) at the cochlear base of fresh human cadaveric specimens. Unlike the classic view, we identified a soft-tissue structure between the BM and OSL in humans, which we name the CP "bridge." We measured CP transverse motion in humans and found that the OSL moved like a plate hinged near the modiolus, with motion increasing from the modiolus to the bridge. The bridge moved almost as much as the BM, with the maximum CP motion near the bridge–BM connection. BM motion accounts for 100% of CP volume displacement in the classic view, but accounts for only 27 to 43% in the base of humans. In humans, the TM–limbus attachment is above the moving bridge, not above a fixed structure. These results challenge long-held assumptions about cochlear mechanics in humans. In addition, animal apical anatomy (in *SI Appendix*) doesn't always fit the classic view.

hearing | cochlea | inner ear | basilar membrane | tuning

Our understanding of the mechanics of mammalian hearing is founded largely on measurements from the cochlear base of laboratory animals such as mouse, gerbil, guinea pig, chinchilla, and cat. The results on humans presented here overturn the widely held belief that the pattern of motion of the cochlear partition (CP) is similar across mammals.

The cochlea is divided into 2 fluid-filled compartments by the CP, which, in the generalized classic view, consists of a rigid osseous spiral lamina (OSL) and an elastic basilar membrane (BM). The classic view is that the frequency-dependent response of the cochlea mostly relies on the vibration of the BM, a thin collagenous membrane that is tuned to high-frequency sounds in the cochlear base and low-frequency sounds in the cochlear apex. Sitting on the BM is the organ of Corti (OoC), which translates BM vibrations into deflections of the stereocilia (or "hairs") of hair cells that amplify BM motion and transduce the motion into the firing of auditory nerve fibers. The classic view has been that BM motion is translated into a shearing motion at the top of the OoC between the reticular lamina and the tectorial membrane (TM), and this shearing deflects hair cell stereocilia (1). Recent studies that were able to measure motion near the reticular lamina, TM, and hair cells have shown that OoC motion is more complex (2–8). Despite the lack of a full detailed understanding of cochlear micromechanics, the belief persists that the basic pattern of CP motion is universal across mammalian species because BM and OoC anatomy are similar across mammals (9).

It is commonly thought that OSL motion in response to sound is negligible, and this is reflected in classic cochlear models that assume there is no OSL motion (10–13). Additionally, the attachment of the OSL to the BM and the attachment of the TM to the spiral limbus (which sits above the OSL) are also considered stationary. In contrast to this view, there have been reports of sound-induced OSL movement, but these reports have been largely ignored in overviews of cochlear mechanics and the formation of cochlear models (10–13). Von Békésy (14), using static pressure, found that the CP "bent like an elastic rod that was free at one end and fixed at the other". Kohlloeffel (15) described the OSL as short and stiff in cat, rat, guinea pig, gerbil, squirrel monkey and rabbit, but as fragile and flexible in pig, cow, and mole, and that, in humans, the OSL can deflect as much as the BM in response to low-frequency sound. Most of the early papers that measured BM responses to sound in live animals using quantitative measuring techniques made control measurements of nearby OSL motion and found that OSL motion was small compared with BM motion at best frequency (BF), although, below BF, OSL motion was sometimes said to be only 5 dB less than BM motion (e.g., refs. 16 and 17). Recent measurements in a human temporal bone found that, in response to air-conducted sound, the OSL vibrated transversely with amplitudes comparable to those of the BM (18), but these measurements were only made at 2 points on the OSL for 1 specimen, and were not intended to establish the overall motion of the OSL or its consequences. The finding of substantial OSL motion in live animals and in a human cadaver conflicts with the generalized classic view that the OSL and the structures that attach above it are basically stationary. Although there have been a number of reports of OSL

Significance

Basic properties of hearing such as its sensitivity and frequency tuning arise from the mechanical responses in the cochlea. Such responses have been measured extensively in the cochlear base of laboratory mammals, and our understanding of human cochlear mechanics is largely founded on the assumption that cochlear mechanics is similar in all mammals. Here we show that the anatomy and motion of the human cochlear partition differ in crucial ways from the generalized classic view of mammalian cochlear mechanics. Our results call into question this classic view. Establishing the features of human cochlear anatomy and function is important for understanding human hearing and for comparison with results from laboratory animals.

Author contributions: S.R. and H.H.N. designed research; S.R. and H.H.N. performed research; S.R., J.J.G., and H.H.N. analyzed data; and S.R., J.J.G., and H.H.N. wrote the paper.

The authors declare no conflict of interest.

This article is a PNAS Direct Submission. C.A.S. is a guest editor invited by the Editorial Board.

Published under the PNAS license.

[1]To whom correspondence may be addressed. Email: sraufer2@gmail.com.

This article contains supporting information online at www.pnas.org/lookup/suppl/doi:10.1073/pnas.1900787116/-/DCSupplemental.

Published online June 24, 2019.

motion, there has not been a systematic study of the motion of various points across the human CP, or across the OSL in any species.

To better understand the mechanics of hearing in humans, we measured sound-induced motion throughout the CP width in the base of fresh human temporal bones and compared the results with the classic view of cochlear motion. To determine human CP motion, we viewed the CP scala tympani surface through the round window and measured transverse motion at many points across the CP width with laser Doppler vibrometry. To interpret these experiments, we examined CP anatomy from histological sections.

Results

Human CP Anatomy Differs from the Anatomy in the Base of Laboratory Animals. In the base of most laboratory animals, much of cochlear anatomy is similar, in particular, the anatomy of the CP. The bony plates of the OSL extend laterally (toward the spiral ligament) to come close to, or overlap with, the medial edge of the BM, approximately in the region of the inner pillars under the inner hair cells. Cochlear anatomy is shown for the base of guinea pig in Fig. 1*A*, and additionally for 4 other commonly used laboratory animals in *SI Appendix*, Fig. S1. In the cochlear base of laboratory animals such as the guinea pig (Fig. 1*A*), the spiral limbus and its attachment point to the TM rest above the bone of the OSL. In Fig. 1*A*, the BM occupies ∼34% and the bony OSL occupies ∼66% of the CP width.

In contrast, in the base of the human cochlea, the BM occupies ∼15% and the bony OSL occupies ∼70% of the CP width (Fig. 1*B*). In humans, the bony part of the OSL does not come close to the BM. Instead, between the lateral edge of the OSL bone and the medial edge of the BM, there is nonbony tissue that forms a third CP region in addition to the OSL and the BM, which has not been anatomically delineated and which we name the CP bridge (Fig. 1 *B* and *C*). In humans, the attachment point of the TM on the spiral limbus does not rest above the bone of the OSL (as in the base of laboratory animals and in cochlear models), but, instead, rests on bridge tissue between the OSL bone and the BM. A magnified view of the CP bridge is shown in Fig. 1*C*. We define the boundaries of the bridge as the bony OSL (medially), the limbus (toward scala vestibuli), the BM (laterally), and the abutting fluid (toward scala tympani). Within the bridge region are connective tissue and auditory nerve fibers. The boundary between the bridge, the limbus, and the inner sulcus needs further examination and definition. The name "tympanic lip" has been used for the lower border of the inner sulcus (19) without regard to whether it is above bone or not. The bridge spans a substantial width. In the cochlear base, the width of the bridge was 83 ± 12% SD of the BM width across 6 histologically prepared temporal bones. The bridge is present in all turns of the human cochlea and has approximately the same width as the BM (both become wider in the apex).

Human CP Motion Is Substantially Different from the Classic View of CP Motion. A representative example of the normalized velocity of the human CP, measured at 34 radial locations across the CP tympanic surface, for frequencies below and near the BF, is shown in Fig. 2. The measurements were normalized to the maximum velocity of the CP at each frequency (Fig. 2*A*) or to the intracochlear pressure measured in the vestibule (Fig. 2 *B*–*D*). The normalized CP responses were independent of the tested stimulus levels of 80 to 120 dB sound pressure level (SPL) at the ear canal.

In response to sound, the human OSL was not stationary (as in classic models), but moved almost as much as the BM. The displacement of the OSL increased linearly with radial distance from a pivot point near the modiolus (at a radial location of −600 μm from the OSL–bridge boundary in Fig. 2*A*). In the CP bridge region medial to the inner sulcus (IS in Fig. 1*C*), the motion of the bridge was continuous with that of the OSL, meaning that the velocity continued to increase linearly with the distance from the modiolus. In the more lateral bridge region near the inner sulcus (between the limbus and BM), the motion usually became greater than a simple extension of the OSL pivoting motion (Fig. 2*A*). The largest transverse CP motion was generally on the BM near the BM–bridge boundary, close to where the inner pillars and inner hair cells are located (IP in Fig. 2*A*). Lateral to the CP motion peak, the motion decreased to a stationary point where the BM attached to the spiral ligament (SL in Fig. 1*A*).

Fig. 3 shows CP motion in all 6 temporal bones. In all, the OSL and bridge moved in response to sound, including the regions of the BM–bridge attachment and underneath the TM–limbus attachment. On average across the 6 temporal bones, the BM accounted for 27.2 ± 7.7% SD of the total transverse area displacement of the CP for frequencies below BF, and 42.7 ± 26.6% SD of the CP area displacement at the BF. This contrasts with classic models in which BM motion is ∼100% of CP area displacement. Overall, in all 6 human temporal bones, OSL and bridge motion accounted for a substantial fraction of the CP area displacement at all tested frequencies.

At frequencies below BF, the whole CP vibrated in phase with deviations of only a few degrees (pink and purple lines in Fig. 2*B* and *SI Appendix*, Fig. S3). At frequencies near BF, and particularly above BF, the phase in the bridge and BM regions sometimes lagged the phase in the OSL region (black and green lines in Fig. 2*B* and *SI Appendix*, Fig. S3). These data suggest that, near and above the BF, there can be phase differences between the OSL, bridge, and BM. CP phase changed with frequency, as shown by the separation of lines in Fig. 2*B*; this phase–frequency relationship is examined in the next section.

Similar Tuning Characteristics of the OSL, Bridge, and BM. The OSL, CP bridge, and BM all had similar frequency response tuning (Fig. 2*C* and *SI Appendix*, Fig. S3). Across temporal

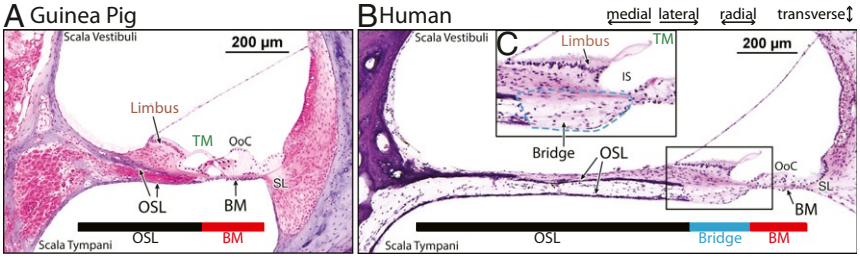

Fig. 1. Cross-sectional anatomy of guinea pig and human CPs. Colored bars show the radial extents of the OSL, the BM, and, in humans, the soft tissue "bridge" between the OSL and BM. (*A*) Guinea pig 10-kHz place (5.5 mm from the base) and (*B*) human 9-kHz place (6 mm from the base). (*C*) Magnified view showing the bridge region outlined with a dashed blue line. Other abbreviations are inner sulcus (IS) and spiral ligament (SL).

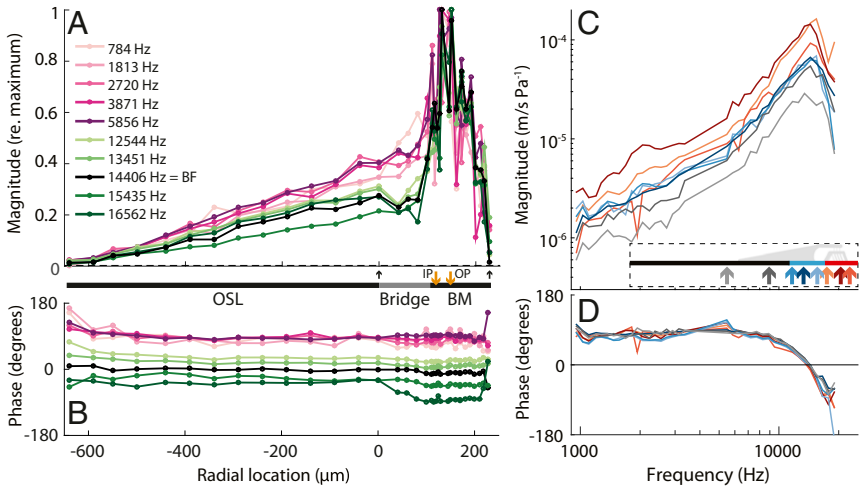

Fig. 2. CP cross-sectional motion profiles and tuning curves. (*A*) Normalized CP transverse velocity magnitude versus radial location in response to tones over a wide range of frequencies (see frequency color key) for a representative temporal bone (#16). Velocity was normalized by the maximum velocity at each frequency. Upward arrows indicate the lateral edge of the OSL at 0 μm and the lateral edge of the BM at 230 μm. The thick line between *A* and *B* estimates the widths of CP structures; the orange arrows indicate the estimated locations of the bottoms of the inner pillar (IP) and outer pillar (OP). (*B*) CP transverse velocity phase referenced to the intracochlear vestibule pressure phase. (*C*) CP motion tuning-curve magnitudes and (*D*) phases referenced to vestibule pressure, at different radial locations (location color key shown on diagram in *C*). The BF of the BM was 14.4 kHz. Data were recorded for ear canal sound pressure levels of 108 dB SPL.

bones, the BFs of the BM ranged from 9.5 to 14.4 kHz. On average, the passive human BM tuning sharpness, measured by Q_{10} (Q_{10} is defined as the BF divided by the bandwidth at which the peak sensitivity decreased by 10 dB), was 1.6 ± 0.5 SD, which is similar to the Q_{10} of passive BM motion in other species, including guinea pig, Q_{10} = 1.4 at BF 25 kHz (20); gerbil, Q_{10} = 2.1 at BF 33 kHz (21); chinchilla, Q_{10} = 1.3 to 1.6 at BF 6 kHz (22); and mouse, Q_{10} = 1.1 to 1.8 at BF 3 to 4.4 kHz (3, 4, 7). Our basal BM tuning is also similar to more apical (12 mm from the base) human passive BM tuning sharpness as reported by Stenfelt et al. (18) Q_{10} = 1.0 and Gundersen et al. (23) Q_{10} = 2.44. In our data, the bridge Q_{10} was 1.16 ± 0.34 (SD), and the OSL Q_{10} was 1.10 ± 0.27 (SD). Although, across specimens, there was a trend that tuning slightly sharpened from OSL to bridge and BM, none of these changes reached statistical significance at $P < 0.05$ (t test) in our small population from different BFs.

For all locations across the CP, the response phase became more delayed as stimulus frequency increased. At the highest frequencies, sometimes there's a hint that the phase plateaued (Fig. 2*D* and *SI Appendix*, Fig. S3). This pattern is consistent with that of a traveling wave, i.e., as frequency increased, phase delays increased slowly at low frequencies and quickly near BF frequencies. This is evidence for traveling waves on the BM, and also on the OSL and the bridge.

Discussion

Our findings provide a picture of the human CP that is substantially different from the classic view of the CP derived from the base of laboratory animals and accepted as almost universal among mammals. First, our observation of human CP anatomy in terms of its effect on function has led us to distinguish a third CP region between OSL and BM, the CP bridge. The bridge might have been considered as part of the OSL, but, unlike the OSL (osseous or bony spiral lamina), it contains no bone. Most small laboratory animals do not show a bridge-like region in the cochlear base (*SI Appendix*, Fig. S1), and such a region is not included in classic cochlear models. Although classic models are assumed to apply to the apex as well as the base, even in laboratory animals, there can be a bridge-like region in the apical CP (*SI Appendix*, Fig. S2). Second, since the BM traveling wave depends on its coupling with cochlear fluid motion, the additional fluid displacement by the OSL and bridge motion might have substantial impact on cochlear tuning and amplification, both of which involve the traveling wave. Finally, and perhaps most importantly, the radial profile of BM transverse motion in humans is different in key ways from the classic view. In particular, the regions where the BM attaches to the bridge and the TM attaches to the limbus move in humans but are considered stationary in classic cochlear models. Our data show that, in this aspect of cochlear mechanics, and perhaps in other aspects such as tuning, the classic view of cochlear mechanics does not apply to the base of humans. *SI Appendix*, Fig. S2 shows that the classic view is also inconsistent with the apical anatomy of a number of small laboratory animals. Whether anatomy and cochlear

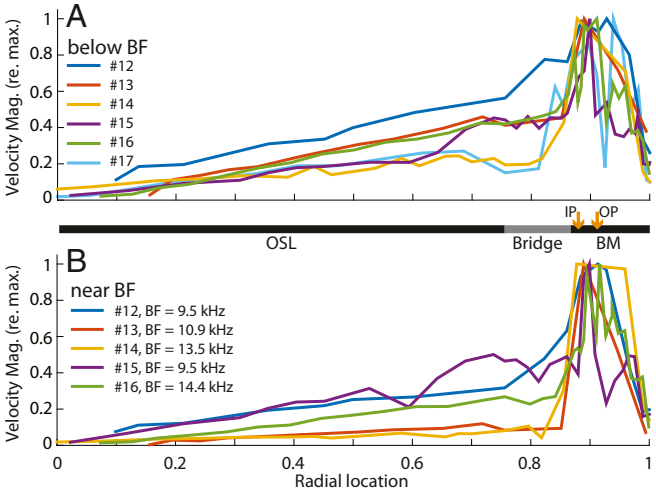

Fig. 3. Motion of the CP referenced to maximum motion. (*A*) Average velocity below BF for each specimen (n = 6). (*B*) Average velocity near BF from each specimen (n = 5; see *SI Appendix*, Fig. S3 for more data.) The overall CP width was normalized to be from 0 to 1. Orange arrows indicate the estimated locations of the bottoms of the IP and OP. Ear canal sound was between 98 and 110 dB SPL (details in *SI Appendix*). Mag., magnitude.

motions in the base of larger mammals, or mammals more closely related to humans (e.g., primates), are similar to humans remains to be determined (for related work, see refs. 16, 24, and 25). Further, the sharper cochlear tuning found in humans compared with laboratory animals (25–27) may be related to our findings, but this remains to be determined.

Our CP motion measurements were made in the base of the cochlea, which is tuned to high frequencies. Our anatomical study on histological sections from 21 human temporal bones shows that the bridge is present in all specimens. Also, the BM and bridge width are approximately the same and increase from base to apex. Additionally, the human OSL movement reported by Stenfelt et al. (18) was from the 2-kHz cochlear region, which shows that human OSL movement is not restricted to the cochlear base. Considering these observations, the overall pattern of OSL and bridge motion we have seen in the base is likely present throughout the human cochlea. This does not rule out there being differences in cochlear motions between base and apex as has been found in laboratory animals (5, 6, 8).

Comparison to Other Studies. Previous studies of human CP anatomy have described aspects of the CP bridge, but these studies were not focused on structural relevance to dynamics and did not clearly delineate the CP bridge from other structures (19, 28, 29). The first reported quantitative measurements of OSL motion in a human temporal bone was by Stenfelt et al. (18). In 1 specimen, they measured at points near the modiolus (OSL1), near the lateral edge of the OSL (OSL2), and on the BM. However, they did not distinguish a CP bridge region and made no mention of how they decided where their measurement points were relative to the detailed anatomy (18). Stenfelt et al.'s measurements were near the 2-kHz BF place, while ours were near the 9- to 15-kHz BF places. These factors prevent us from being able to make a detailed comparison of their results and ours. However, Stenfelt et al.'s measurements are consistent with ours in that the magnitude of motion of the OSL was comparable to that of the BM, and that both BM and OSL phase patterns were appropriate for these structures to be carrying traveling waves.

Several studies in animals have reported measurements of sound-induced motion at different radial positions across the BM and sometimes from the OSL (reviewed in the Introduction). Reports from most animal experiments found minimal BM motion at its attachment to the OSL and the largest transverse motion in the region from the outer pillars to the center of the BM, with only small differences in the phase seen at different BM locations (5, 30, 31). One exception is the studies of Nilsen and Russell (32), who made measurements with a self-mixing laser and reported that the largest motions were near the outer pillars, but they also reported large phase differences (up to 180°) for small variations in radial position. The different results of Nilsen and Russell can be accounted for by the possibility that their method included motion of deep structures of the OoC, rather than just the surface motion of the BM. For a more detailed discussion, see ref. 33.

Implications of Measurements from a Fresh Cadaveric, Passive Preparation. Passive-cochlea data are important for understanding human CP motion at high sound levels, or when active processes cease to work (e.g., in sensorineural hearing loss), and as an important foundation to understand CP motion with cochlear amplification.

Most animal studies have found no differences in the shape of the radial profile of BM transverse motion between active and passive cochleas (30), but whether this holds for humans is unknown. In an active cochlea, outer hair cells (OHCs) produce cochlear amplification by adding energy to the traveling wave (34). In the long-wave region of the traveling wave, which is basal to the BF region, the sound pressure is close to uniform in a transverse section across the cochlear scalae and would affect the OSL, bridge, and BM regions similarly. However, in the short-wave region near the BF, experiments and models of cochlear mechanics suggest that the sound pressure spread away from the BM may be spatially limited (12, 35), which may cause the OSL and bridge regions to move differently than the BM.

Another possible limitation of our measurements is that CP tissue properties may change substantially after death. Although we have seen no indication of this from our measurements over hours if the CP was kept moist, time effects cannot be ruled out, because our earliest measurements were 47 h postmortem. Many animal studies of BM motion before and shortly after death have shown a large initial motion decrease near BF (and a change in BF) from the loss of cochlear amplification, but, over the next few hours, only small changes occurred. Over longer periods after death, BM stiffness decreased (36, 37) and low-frequency BM motion increased (38), but, at 16 h postmortem, the shape of the cross-sectional motion profile was not affected (30). In mice, TM material properties and TM traveling waves were similar at 1 h versus 48 h postmortem, and are similar to those of postmortem human TMs (39). These experiments used cold, moist (never frozen) storage, as was done in our present study. Human cochlear input impedance from intraoperative measurements in live cochleas was similar to that in cadaveric temporal bones, which suggests that overall CP properties did not grossly change after death (40). Our measurements of CP motion in passive human cochleas are the freshest yet made, but may not be the same as just after death.

Modeling Human CP Motion. We found that the low-frequency cross-sectional motion of the CP can be described by a composite beam model with 2 elements: a rigid rod hinged near the modiolus (emulating the OSL and the medial half of the CP bridge) and a flexible beam with constant bending stiffness, simply supported at both ends (emulating the lateral part of the CP bridge and the BM). This model, described in *SI Appendix*, captures the overall properties of our CP motion measurements: 1) The OSL moves as a stiff plate hinged near the modiolus, 2) the motion is large in the bridge region under the attachment of the TM to the limbus and where the BM attaches to the bridge, and 3) the maximum CP motion occurs near the BM–bridge connection.

There are 2 other modeling studies that are relevant in that their CPs included both a rigid part and a flexible part [Kapuria et al. (41) and Taber and Steele (42); see *SI Appendix*]. In these models, the volume displacement of the near-rigid region was large compared with that of the flexible BM region, but the near-rigid region had relatively little influence on the shape and BF of the traveling wave, except for delaying the phase. These results may imply that the presence of a large fluid volume displacement by the OSL and bridge in humans may have little effect on BF characteristics set by the BM. However, these models did not include cochlear micromechanics, in particular, the mechanical drives to hair cell stereocilia, where major effects due to a mobile OSL and bridge might be expected.

Implications of the Human CP Motion Profile. To understand how CP motion may relate to the motion of structures within the OoC, we consider simplified cross-sectional diagrams of the anatomy and low-frequency motion of the CP and OoC (Fig. 4). The classic view of BM and OoC motion is shown in Fig. 4*A*. As the BM moves up (toward scala vestibuli), the OoC rotates counterclockwise about the bottom of the inner pillars, with BM motion greatest around the outer pillars, OHCs, and the center of the BM. The resulting rotation of the TM about a stationary origin at the attachment to the limbus produces little radial motion of the TM at the TM attachment to OHC stereocilia. It has been hypothesized that the TM has substantial radial motion

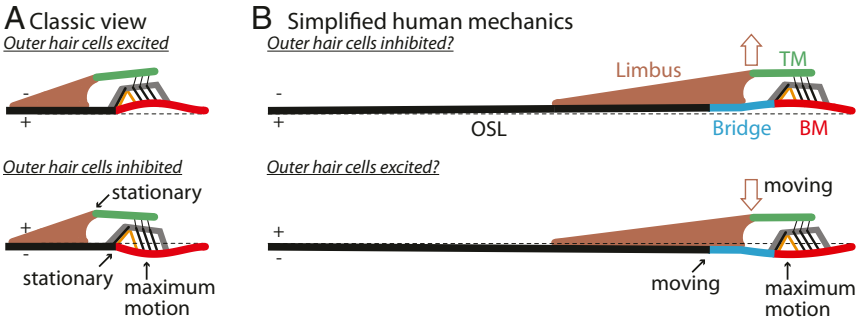

Fig. 4. Simplified diagrams of CP anatomy and motion for low frequencies. (*A*) In the classic model, the OSL and the limbus are stationary while the BM and OoC (structures above the BM) move in response to a sound pressure difference across the partition (depicted by +/−). (*B*) In the human cochlear base, the BM and OoC move, and, also, the OSL and bridge (including the attachments of the TM to the limbus) move in response to sound.

due to a TM mass–stiffness resonance (e.g., refs. 43 and 44). However, measurements show that the TM is viscoelastic, with large damping without sharp resonance, and the TM can carry longitudinally propagating traveling waves of radial motion (45). Theoretical studies implicate the importance of both the TM propagation and heavily damped TM resonance (11). The longitudinally carried TM radial motion may be more important than TM resonances, but in vivo TM motion is poorly understood and is likely different from the classic view. In addition, recent experiments show that the reticular lamina moves much more than the BM, and there is differential motion between structures at the top of the OoC, such as rotation of the reticular lamina (2–8, 46). All of the above indicate that the classic view in Fig. 4*A* needs modification, and some models do incorporate more complex motions at the top of the OoC. Nonetheless, no new view has been widely accepted that replaces the classic view (Fig. 4*A*) that the counterclockwise rotation of the OoC moves the reticular lamina (at the OHC stereocilia) radially toward the modiolus, which deflects OHC stereocilia in the excitatory direction. Whatever the variations at the top of the OoC, most models (except ref. 42) assume that the edges of the BM are stationary and that the attachment of the TM at the limbus is stationary.

Fig. 4*B* shows a recasting of the diagram of Fig. 4*A* for the anatomy of the human CP and for low-frequency motion. The CP motion facing scala tympani is based on our measurements and model (*SI Appendix*, Fig. S4). The illustrated motion of the structures around the OoC is a simple extrapolation from our measured CP motion. In contrast to the classic view of CP motion, in humans, the CP has substantial transverse motion in the region under the TM–limbus attachment and at the BM–bridge attachment, and has the greatest transverse motion near the inner pillar medial to the outer pillar/OHCs. In upward BM motion, the BM–bridge attachment moves upward so that the OoC rotates clockwise (Fig. 4*B*)—opposite to the rotation of the classic view (Fig. 4*A*). This opposite rotation moves the reticular lamina radially away from the modiolus, which would deflect OHC stereocilia in the inhibitory direction. Furthermore, in humans, the TM–limbus attachment, which is stationary in the classic view, is expected to move because it sits on a CP bridge region that moves. If the limbus rotates in a counterclockwise direction for upward BM movement (as in Fig. 4*B*), it would produce radial TM motion toward the modiolus, and this radial TM motion would further deflect OHC stereocilia in the inhibitory direction. Fig. 4 is for low-frequency motion, but, for frequencies near BF, fluid and tissue inertia will change the motion (47). As noted in the previous paragraph, the radial motion of the TM is unknown, and the motions at the top of the OoC are likely to be more complicated than in the classic view. Nonetheless, the contrast between the CP motions in the classic view (Fig. 4*A*) versus the simple extrapolation of our human CP measurements (Fig. 4*B*) shows the highly consequential functional implications of the differences in CP motion.

One major difference at the top of the OoC between the classic view and our findings in humans is in TM motion (Fig. 4). In the classic view, the TM–limbus attachment is stationary, and motion of the TM is produced only by the motion of OHC stereocilia and fluid in the subtectorial space. In humans, the CP limbus region has transverse movement (due to motion of the OSL and bridge), which implies that the TM–limbus attachment point moves, so that, in humans, both ends of the TM are attached to moving structures. Vibration of one end of the TM can be carried to the other radial end, and also carried longitudinally along the TM (45). Thus, TM motion in humans appears to be more complex than in the classic view of cochlear mechanics. An attractive hypothesis is that the different gross OoC motions in Fig. 4*A* vs. Fig. 4*B* are at least partly compensated by different TM motion so that, for upward BM motion, OHC deflections are similar in humans and other species. This speculative hypothesis needs testing.

Cochlear mechanics is the origin of important basic properties of hearing such as hearing sensitivity and frequency tuning. The classic view of cochlear anatomy and mechanics was derived from measurements in the base of extensively studied small animals. Here we have shown that both the anatomy and sound-evoked motion of the human CP differ in crucial ways from the classic view. Our results provide a new perspective on cochlear mechanics in humans. In addition, *SI Appendix*, Fig. S2 suggests that the classic view may also not apply in the apex of some laboratory animals. Understanding the mechanical differences between the human cochlea and those of other species will aid in interpreting results from laboratory animals and properly using them to understand human hearing.

Materials and Methods

Detailed methods are described in *SI Appendix*. In brief, the CP motion measurements were from 6 human (53 to 78 y old, mean = 60.2 y) cadaveric temporal bone specimens, 47 to 108 h postmortem. The CP was viewed through the round window after removing its membrane. The fluid in scala tympani was drained to a thin film over the CP. Measurements used a laser Doppler vibrometer focused directly on the CP, using the tissue's reflected light. Acoustic pure tones between 100 Hz and 24 kHz were delivered to the ear canal. Fiber optic pressure sensors were used to record sound pressure in the vestibule (35, 48). Anatomy was quantified from histological preparations of human specimens and several animal specimens from the Otopathology Laboratory at our institution. All motion data are provided in *SI Appendix*.

ACKNOWLEDGMENTS. We thank Diane Jones, the Massachusetts Eye and Ear (MEE) Otopathology staff, and Mike Ravicz for technical support; Cornelia Idoff for helping with anatomical measurements; and Garyfallia Pagonis for helping design Fig. 1 and *SI Appendix*, Figs. S1 and S2. We

thank Dennis Freeman and Sunil Puria for discussions and manuscript comments, and 2 anonymous reviewers for helpful suggestions. This work was supported by National Institutes of Health/National Institute on Deafness and Other Communication Disorders Grant R01DC013303, fellowships from the German National Academic Foundation and the American Otological Society, and an Amelia Peabody scholarship from MEE.

1. E. ter Kuile, Die Uebertragung der Energie von der Grundmembran auf die Haarzellen. *Archiv fuer die Gesammte Physiologie des Menschen und der Thiere* **79**, 146–157 (1900).
2. NP Cooper, A. Vavakou, M. V. D. Heijden, Vibration hotspots reveal longitudinal funneling of sound-evoked motion in the mammalian cochlea. *Nat. Commun.* **9**, 3054 (2018).
3. H. Y. Lee *et al.*, Two-dimensional cochlear micromechanics measured in vivo demonstrate radial tuning within the mouse organ of Corti. *J. Neurosci.* **36**, 8160–8173 (2016).
4. T. Ren, W. He, W. Kemp, Reticular lamina and basilar membrane vibrations in living mouse cochleae. *Proc. Natl. Acad. Sci. U.S.A.* **113**, 9910–9915 (2016).
5. R. L Warren *et al.*, Minimal basilar membrane motion in low-frequency hearing. *Proc. Natl. Acad. Sci. U.S.A.* **113**, E4304–E4310 (2016).
6. A. Recio-Spinoso, J. S Oghalai, Mechanical tuning and amplification within the apex of the Guinea pig cochlea. *J. Physiol.* **595**, 4549–4561 (2017).
7. H. Y. Lee *et al.*, Noninvasive in vivo imaging reveals differences between tectorial membrane and basilar membrane traveling waves in the mouse cochlea. *Proc. Natl. Acad. Sci. U.S.A.* **112**, 3128–3133 (2015).
8. W. Dong *et al.*, Organ of Corti vibration within the intact gerbil cochlea measured by volumetric optical coherence tomography and vibrometry. *J. Neurophysiol.* **120**, 2847–2857 (2018).
9. S. Narayan, A. N. Temchin, A. Recio, M. Ruggero, Frequency tuning of basilar membrane and auditory nerve fibers in the same cochleae. *Science* **282**, 1882–1884 (1998).
10. C. R. Steele, J. B. de Monvel, S. Puria, A multiscale model of the organ of Corti. *J. Mech. Mater. Struct.* **4**, 755–778 (2009).
11. J. Meaud, K. Grosh, The effect of tectorial membrane and basilar membrane longitudinal coupling in cochlear mechanics. *J. Acoust. Soc. Am.* **127**, 1411–1421 (2010).
12. G. Zweig, Nonlinear cochlear mechanics. *J. Acoust. Soc. Am.* **139**, 2561–2578 (2016).
13. E. de Boer, A. L. Nuttall, C. A. Shera, Wave propagation patterns in a "classical" three-dimensional model of the cochlea. *J. Acoust. Soc. Am.* **121**, 352–362 (2007).
14. G. von Bekesy, *Experiments in Hearing* (Acoustical Society of America, 1960).
15. L. U. E. Kohlloeffel, "Problems in aural sound conduction" in *Mechanics of Hearing-Proceedings of the IUTAM/ICA Symposium*, E. de Boer, M. Viergever, Eds. (Martinus Nijhoff Publishers, 1983), pp. 211–217.
16. S. Rhode, Observations of the vibration of the basilar membrane in squirrel monkeys using the mossbauer technique. *J. Acoust. Soc. Am.* **49**, 1281–1231 (1971).
17. W. S. Rhode, Basilar membrane mechanics in the 6–9kHz region of sensitive chinchilla cochleae. *J. Acoust. Soc. Am.* **121**, 2792–2804 (2007).
18. S. Stenfelt, S. Puria, N. Hato, R. L. Goode, Basilar membrane and osseous spiral lamina motion in human cadavers with air and bone conduction stimuli. *Hearing Res* **181**, 131–143 (2003).
19. S. N. Merchant, J. Nadol, *Schuknecht's Pathology of the Ear*, S. N. Merchant, J. Nadol, Eds. (PMPH, ed. 3, 2010).
20. N. P Cooper, W. S. Rhode, Basilar membrane mechanics in the hook region of cat and Guinea-pig cochleae: Sharp tuning and nonlinearity in the absence of baseline position shifts. *Hearing Res.* **63**, 163–190 (1992).
21. W. Dong, E. S. Olson, In vivo impedance of the gerbil cochlear partition at auditory frequencies. *Biophysical J* **97**, 1233–1243 (2009).
22. A. Recio, N. C. Rich, S. S. Narayan, M. A. Ruggero, Basilar-membrane responses to clicks at the base of the chinchilla cochlea. *J. Acoust. Soc. Am.* **103**, 1972–1989 (1998).
23. T. Gundersen, O. Skarstein, T. Sikkeland, A study of the vibration of the basilar membrane in human temporal bone preparations by the use of the mossbauer effect. *Acta Oto-Laryngologica* **86**:225–232 (1978).
24. P. X. Joris *et al.*, Frequency selectivity in Old-World monkeys corroborates sharp cochlear tuning in humans. *Proc. Natl. Acad. Sci. U.S.A.* **108**, 17516–17520 (2011).
25. C. J. Sumner *et al.*, Mammalian behavior and physiology converge to confirm sharper cochlear tuning in humans. *Proc. Natl. Acad. Sci. U.S.A.* **115**, 11322–11326 (2018).
26. C. A. Shera, J. J. Guinan, A. J. Oxenham, Revised estimates of human cochlear tuning from otoacoustic and behavioral measurements. *Proc. Natl. Acad. Sci. U.S.A.* **99**, 3318–3323 (2002).
27. S. Raufer, S. Verhulst, Otoacoustic emission estimates of human basilar membrane impulse response duration and cochlear filter tuning. *Hearing Res.* **342**:150–160.(2016).
28. A. Corti, *Recherches sur l'organe de l'ouïe des mammiferes* (*Zeitschrift fuer wissenschaftliche Zoologie*, Akademische Verlagsgesellschaft Geest und Portig, 1854), vol. 3.
29. K. Neubert, Die Basilarmembran des Menschen und ihr Verankerungssystem. *Z. für Anatomie Entwicklungsgeschichte* **114**:540–590 (1950).
30. N. P. Cooper, "Radial variation in the vibrations of the cochlear partition" in *Recent Developments In Auditory Mechanics*, H. Wada T. Takasaka, K. Ikeda, K. Ohyama, Eds. (World Scientific, 2000), pp. 109–115.
31. W. S. Rhode, A. Recio, Study of mechanical motions in the basal region of the chinchilla cochlea. *J. Acoust. Soc. Am.* **107**, 3317–3332 (2000).
32. K. E. Nilsen, I. J. Russell, The spatial and temporal representation of a tone on the Guinea pig basilar membrane. *Proc. Natl. Acad. Sci. U.S.A.* **97**, 11751–11758 (2000).
33. J. J. Guinan, Olivocochlear efferents: Their action, effects, measurement and uses, and the impact of the new conception of cochlear mechanical responses. *Hearing Res.* **362**, 38–47 (2018).
34. E. de Boer, A. L. Nuttall, The "inverse problem" solved for a three-dimensional model of the cochlea. III. Brushing-up the solution method. *J. Acoust. Soc. Am.* **105**, 3410–3420 (1999).
35. E. S. Olson, Intracochlear pressure measurements related to cochlear tuning. *J. Acoust. Soc. Am.* **110**, 349–367 (2001).
36. R. C. Naidu, D. C. Mountain, Measurements of the stiffness map challenge a basic tenet of cochlear theories. *Hearing Res.* **124**, 124–131 (1998).
37. L. U. E. Kohlloeffel, A study of basilar membrane vibrations. III. The basilar membrane frequency response curve in the living Guinea pig. *Acustica* **27**, 82–89 (1972).
38. W. S. Rhode, "An investigation of postmortem cochlear mechanics using the Mössbauer effect" in *Basic Mechanisms of Hearing*, A. R. Møller, Ed. (Academic Press, New York, 1973), pp. 49–67.
39. S. Farrahi, R. Ghaffari, J. Sellon, H. Nakajima, D. Freeman, Tectorial membrane traveling waves underlie sharp auditory tuning in humans. *Biophysical J.* **111**, 921–924 (2016).
40. W. Chien *et al.*, Measurements of stapes velocity in live human ears. *Hearing Res.* **249**, 54–61 (2009).
41. S. Kapuria, C. R. Steele, S. Puria, Unraveling the mystery of hearing in gerbil and other rodents with an arch-beam model of the basilar membrane. *Scientific Rep* **7**, 228 (2017).
42. A. Taber, C. R. Steele, Cochlear model including three-dimensional fluid and four modes of partition flexibility. *J. Acoust. Soc. Am.* **70**, 426–436 (1981).
43. J. B. Allen, Cochlear micromechanics-A physical model of transduction. *J. Acoust. Soc. Am.* **68**, 1660–1670 (1980).
44. J. J. Zwislocki, Theory of cochlear mechanics. *Hearing Res.* **2**, 171–182 (1980).
45. R. Ghaffari, A. J. Aranyosi, D. M. Freeman, Longitudinally propagating traveling waves of the mammalian tectorial membrane. *Proc. Natl. Acad. Sci. U.S.A.* **104**, 16510–16515 (2007).
46. M. Nowotny, A. W. Gummer, Nanomechanics of the subtectorial space caused by electromechanics of cochlear outer hair cells. *Proc. Natl. Acad. Sci. U.S.A.* **103**, 2120–2125 (2006).
47. A. W. Gummer, W. Hemmert, H. P. Zenner, Resonant tectorial membrane motion in the inner ear: Its crucial role in frequency tuning. *Proc. Natl. Acad. Sci. U.S.A.* **93**, 8727–8732 (1996).
48. H. H. Nakajima *et al.*, Differential intracochlear sound pressure measurements in normal human temporal bones. *J. Assoc. Res. Otolaryngol.* **10**, 23–36 (2009).